

NASA TECHNICAL NOTE



NASA TN D-5079

c. 1

NASA TN D-5079



LOAN COPY: RETURN TO  
AFWL (WLIL-2)  
KIRTLAND AFB, N MEX

# IMPURITY PROFILE AND ENERGY BAND DIAGRAM FOR THE CUPROUS SULFIDE — CADMIUM SULFIDE HETEROJUNCTION

*by Henry W. Brandhorst, Jr.*

*Lewis Research Center  
Cleveland, Ohio*

## ABSTRACT

Capacitance measurements were used to determine the impurity profile for a  $\text{Cu}_2\text{S}$ -CdS heterojunction formed by acid etching a polycrystalline, evaporated layer of CdS, and dipping it into a cuprous ion solution. Capacitance-voltage measurements were made both in the dark and under illumination. The barrier height of the junction was determined to be 0.85 V. The impurity profile is unaffected by red light, but blue light reduces the compensation of a copper-diffused CdS layer. The capacitance measurements, Hall measurements, and an electron microprobe analysis were used to assemble a band structure for the heterojunction which shows four distinct regions.

# IMPURITY PROFILE AND ENERGY BAND DIAGRAM FOR THE CUPROUS SULFIDE - CADMIUM SULFIDE HETEROJUNCTION

by Henry W. Brandhorst, Jr.

Lewis Research Center

## SUMMARY

The impurity profile in the cadmium sulfide (CdS) layer of the cuprous sulfide-cadmium sulfide ( $\text{Cu}_2\text{S}$ -CdS) heterojunction was determined by capacitance measurements. The heterojunction was formed by acid etching a polycrystalline, evaporated layer of CdS and dipping it into a cuprous ion solution. It was shown that the copper which was diffused into the CdS during a fabrication heat treatment does not completely compensate the excess cadmium centers in the CdS. The net impurity concentration is reduced between two and three orders of magnitude, however. The barrier height was determined to be 0.85 volt, which represents the maximum voltage that can be attained with the heterojunction.

A band structure for the  $\text{Cu}_2\text{S}$ -CdS heterojunction was assembled on the basis of the impurity profile determined from the capacitance measurements and from Hall and electron microprobe measurements on the  $\text{Cu}_2\text{S}$  layer. Apparently, four regions are present in the device: (1)  $n^+$ -type CdS, donor impurity concentration ( $N_d$ ) of approximately  $10^{18}$  per cubic centimeter, Fermi level 0.02 electron volt (eV) below the conduction band edge; (2) n-type CdS:Cu,  $N_d$  of approximately  $10^{16}$  per cubic centimeter, Fermi level 0.13 eV below the conduction band edge; (3) p-type  $\text{Cu}_2\text{S}$ :Cd, acceptor impurity concentration ( $N_a$ ) approximately equal to  $10^{16}$  per cubic centimeter, Fermi level about 0.2 eV above the valence band edge; and (4)  $p^+$ -type  $\text{Cu}_2\text{S}$ ,  $N_a$  approximately equal to  $10^{20}$  per cubic centimeter, near-degenerate  $\text{Cu}_2\text{S}$ , Fermi level at the valence band edge.

The effects of various wavelengths of light on the impurity profile in the CdS were studied. With infrared light, no change occurred in the profile from its dark value. However, blue-green or white light considerably reduced the degree of compensation of the CdS by the copper centers.

## INTRODUCTION

Since the discovery of the photovoltaic effect in cadmium sulfide (CdS) by Reynolds, Leies, Antes, and Marburger (ref. 1), a variety of mechanisms has been proposed for the origin of the effect. Considerable attention has been given to the origin of the anomalous red response, whereas the problem of the type of junction involved has received attention only more recently. The red response has been attributed to impurity band conduction (refs. 2 and 3), photoemission (ref. 4), and electronic excitation in the depletion region of the CdS (refs. 5 to 11). The type of junction said to be present in the device has ranged from a p-n homojunction in the CdS (refs. 5 and 6) to a heterojunction between cuprous sulfide ( $\text{Cu}_2\text{S}$ ) and CdS (refs. 12 to 14).

None of these studies, however, determined the impurity profile or band structure of the heterojunction. The purpose of the present study was to make such measurements in the hope of obtaining a more detailed view of the photovoltaic process in these devices. Of particular interest was the structure of the thin-film  $\text{Cu}_2\text{S}$ -CdS solar cell. Therefore, the heterojunctions studied in this work were formed by acid etching a polycrystalline, evaporated layer of CdS and dipping it into a cuprous ion ( $\text{Cu}^+$ ) solution to produce a layer of  $\text{Cu}_2\text{S}$ . The impurity distribution in the CdS layer was determined with capacitance-voltage measurements. These data, when combined with Hall and electron microprobe information on the  $\text{Cu}_2\text{S}$  layer, allowed the construction of a band diagram for the  $\text{Cu}_2\text{S}$ -CdS heterojunction.

## EXPERIMENTAL PROCEDURE

The cells used in this study were 1- by 2-centimeter thin-film CdS solar cells obtained from the Clevite Corporation. These cells are shown in cross section in figure 1. The CdS layer, formed by vacuum evaporation (ref. 15), has a thickness of about 25 micrometers and a carrier concentration of the order of  $10^{17}$  to  $10^{18}$  per cubic centimeter as determined by Hall measurements. The CdS is n-type with the conductivity coming from excess cadmium. The  $\text{Cu}_2\text{S}$  layer was formed by dipping the acid-etched CdS film into a  $\text{Cu}^+$  solution at  $90^\circ\text{C}$  (363 K) for a few seconds. The p-type layer is degenerate

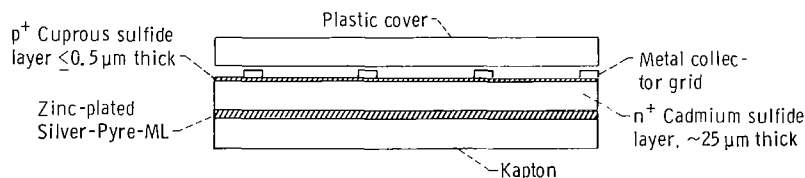


Figure 1. - Cross section of cadmium sulfide thin-film solar cell.

and has a carrier concentration of the order of  $10^{20}$  per cubic centimeter with a maximum thickness of 0.5 micrometer (ref. 16). The cells were then heat treated at  $250^{\circ}\text{C}$  (523 K) for a few minutes to form a good working device. Grids were attached with conductive epoxy cement, and the cells were then laminated in plastic to ensure stability. Cell efficiencies were about 5.0 percent under conditions of air mass 1 illumination and  $25^{\circ}\text{C}$  (298 K).

A Boonton model 75A-S8, 1-megahertz capacitance bridge was used in these studies, and the test arrangement is shown in figure 2. Because the cell impedances were of the order of 5 ohms, a Boonton model 77-2A range extender had to be used. This extender permitted capacitance readings to 100 000 picofarads and impedance readings to 1 ohm. The signal level reaching the sample was approximately 2 millivolts.

Bias voltage was supplied from a stabilized direct-current power supply that, in this test arrangement, delivered 150 milliamperes at 18 volts. The current in the circuit was measured by the voltage drop across a precision 1-ohm resistor which introduced no loading into the circuit. The choke shown in the schematic diagram (fig. 2) was used to

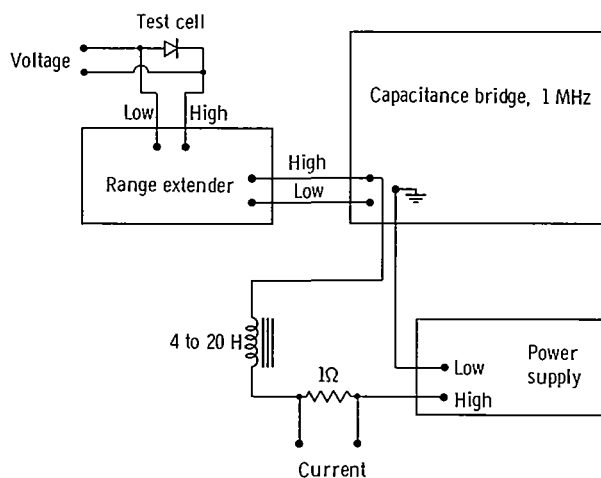


Figure 2. - Capacitance-voltage measurement apparatus.

isolate the power supply from the bridge. The bias voltage across the cell and the voltage across the 1-ohm current-sensing resistor were measured with an integrating digital voltmeter. The input impedance was 1 megohm. The voltmeter was removed from the circuit while the capacitance was being measured to eliminate loading effects.

Large errors in capacitance were noted at sample impedances below 50 ohms. It was therefore necessary to calibrate the test arrangement with known capacitances in parallel with carbon resistors reaching values as low as 1 ohm. This calibration proved satisfactory, and reproducibility of data in these measurements was better than 2 percent.

When capacitance measurements were begun at zero bias and extended to negative bias voltages, unrealistically high barrier heights (in excess of 20 V) were obtained. In addition, the readings were not reproducible because a drift of capacitance with time was noted. Reproducible measurements were obtained only when currents of 100 milliamperes or more were first passed through the cell in the forward ( $\text{Cu}_2\text{S}$  positive) direction. Under these conditions, positive bias voltages in excess of 1 volt were initially obtained; however, the voltage would decay, and stable readings between 0.4 and 0.6 volt were reached after several hours. During this voltage decay, however, no significant change in the capacitance was noted. The conditions of high current flow in the forward direction for long periods of time also caused a large number of cell failures. As the bias voltage was lowered for each successive measurement, it was necessary to wait until stable readings were reached before reproducible data could be obtained.

## THEORY

Schottky (ref. 17) has shown how capacitance-voltage measurements on metal-semiconductor junctions can be used to infer the impurity profile in the semiconductor. In a semiconductor-semiconductor heterojunction, the situation is more complex (ref. 18). However, if one of the semiconductors is heavily doped, most of the depletion region occurs on one side of the junction, and Schottky's theory can be used. This condition is fulfilled for the  $\text{Cu}_2\text{S}$ -CdS heterojunction because the  $\text{Cu}_2\text{S}$  is either degenerate or near-degenerate; hence, most of the depletion region must occur in the CdS. In this situation, Schottky's equations are valid and the impurity concentration can be deduced from the following equation.

$$\frac{d \frac{1}{\left(\frac{C}{A}\right)^2}}{dV} = \frac{2}{\kappa \epsilon_0 e N} \quad (1)$$

where  $C$  is the capacitance,  $A$  is the cell area,  $V$  is the applied bias voltage,  $\kappa$  is the dielectric constant (9 for CdS at 1 MHz and assumed to be independent of doping at the concentrations observed), and  $\epsilon_0$  is the permittivity of vacuum. Inherent in the derivation of equation (1) is the assumption that ionization and recombination processes are not involved, as the impurity centers are completely ionized in the bulk material, and that the space charge due to free carriers is negligible. Under these circumstances,  $N$ , representing the net impurity concentration, can thus be represented by  $N_d$  or  $N_a$ , the donor

or acceptor impurity concentration, respectively, or their difference in the case of impurity compensation. The slope of the line relating  $1/(C/A)^2$  and  $V$  at any applied bias is seen to be inversely proportional to the local net impurity content. This relation holds for any impurity profile, as does the expression for the depletion layer width ( $\lambda$ ):

$$\lambda = \frac{\kappa \epsilon_0 A}{C} \quad (2)$$

## RESULTS

### Impurity Distribution

A typical plot of  $A^2/C^2$  against bias voltage is shown in figure 3. The curve shows two slopes separated by an abrupt transition region. At reverse biases above 3 volts,

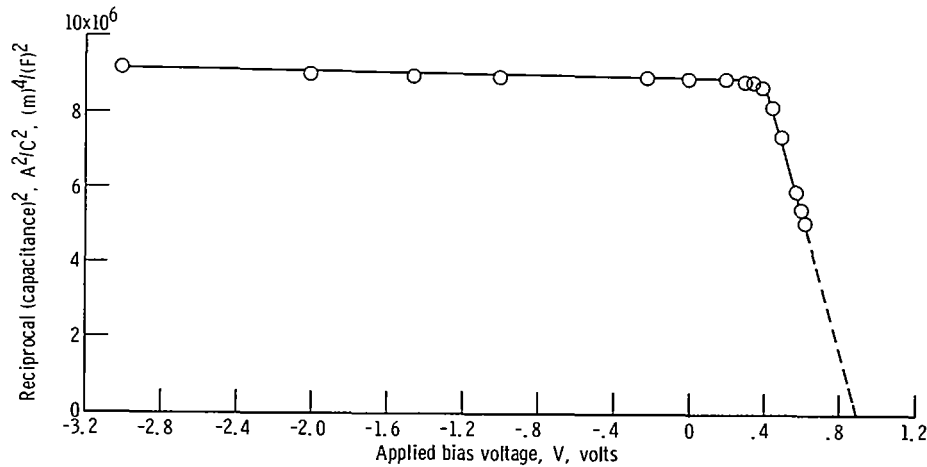


Figure 3. - Capacitance-voltage plot for cuprous sulfide-cadmium sulfide thin-film solar cell B724A-6 (as-received).

deviations from linearity take place which can be caused by breakdown, traps (ref. 19), or the nonuniformity of the junction (ref. 20). Therefore, no analysis was made beyond 3 volts because these effects could not be separated. The impurity profile obtained from equations (1) and (2) is shown in figure 4. The ordinate scale ( $N_d - N_a$ ) represents the net impurity concentration. It can be clearly seen that partial compensation of the bulk CdS has taken place. The acceptor in this case is probably copper that was diffused into the CdS during a heating step in the process of cell fabrication. Figure 4 shows that the

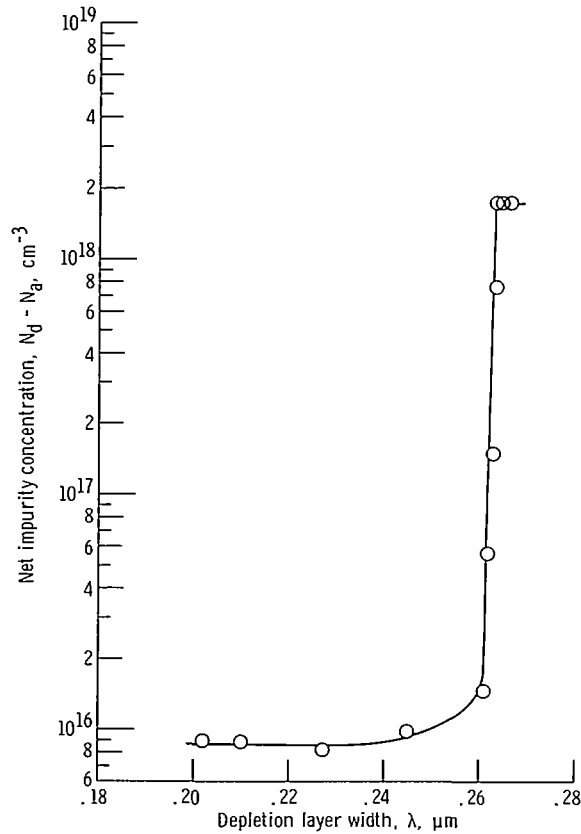


Figure 4. - Impurity distribution in cadmium sulfide layer of cell B724A-6 (as-received).

copper has not completely compensated the CdS because the concentration in the copper-diffused region is about  $9 \times 10^{15}$  per cubic centimeter. The transition in the profile is abrupt and comes at a depth of 0.26 micrometer in the CdS. The impurity concentration in the bulk CdS is about  $2 \times 10^{18}$  per cubic centimeter. Errors introduced by the slope calculation lead to an uncertainty of 10 to 20 percent in the quoted value at doping levels of the order of  $10^{18}$  per cubic centimeter. At the lower net impurity concentrations typical of the copper-diffused CdS, the reproducibility of the concentration values is about 5 percent.

Because the impurity distribution appears to be uniform near the junction, it is possible to extrapolate the line above 0.45 volt to obtain the barrier voltage  $V_D$  of the junction (ref. 20). For the data of figure 3, such an extrapolation yields  $V_D = 0.87$  volt.

The value of the impurity concentration in the bulk CdS as just determined is about one order of magnitude higher than Hall data on similar films. This discrepancy can be attributed to the uncertainty in the junction area. Photomicrographs show that the surface of the cell is quite rough with valleys running down grain boundaries. In this study, the valleys were ignored and the area was determined from the total cell area ( $2 \text{ cm}^2$ ).



nominal) and a geometric roughness measured from photomicrographs. This roughness increases the nominal area by about 10 percent. Quite possibly, the actual cell area may be two to three times greater than this estimate if the valley area were to be included. Using a larger estimate of cell area would simply shift the carrier profile to a greater depth and decrease the carrier concentrations but would not affect the basic conclusions of this report. For the data of figure 4, for example, if the true area were three times greater, the depletion layer width would be 0.79 micrometer, the concentration in the CdS:Cu would be  $10^{15}$  per cubic centimeter and in the bulk CdS,  $2 \times 10^{17}$  per cubic centimeter. These concentrations are about an order of magnitude less than the uncorrected values and correspond well to the Hall data.

The shape of the impurity distribution shown in figure 4 is typical of the diffusion of a compensating impurity into certain crystals. Similar results have been obtained for the diffusion of copper into zinc selenide (ref. 21). Capacitance measurements determine the net charged impurity distribution and not necessarily the atomic diffusion profile. When compensation is occurring in the II-VI compounds, there will be an abrupt change in the net charged impurity concentration when the concentration of the compensating impurity falls below the donor (or acceptor) concentration in the host crystal.

## Heat Treatment

A brief heat treatment at  $200^{\circ}\text{C}$  (473 K) was given the cell to determine whether or not a shift in the impurity profile would occur because of further diffusion. The results are presented in figure 5, which shows that the impurity concentration in the bulk CdS remained the same while the transition region moved deeper into the cell. The degree of compensation of the CdS:Cu layer has also increased and further increases with increasing time and temperature of the heat treatment. For example, in a test on another cell, a 10-minute heat treatment at  $230^{\circ}\text{C}$  (503 K) lowered the impurity concentration in the CdS:Cu layer from approximately  $10^{16}$  to  $10^{15}$  per cubic centimeter.

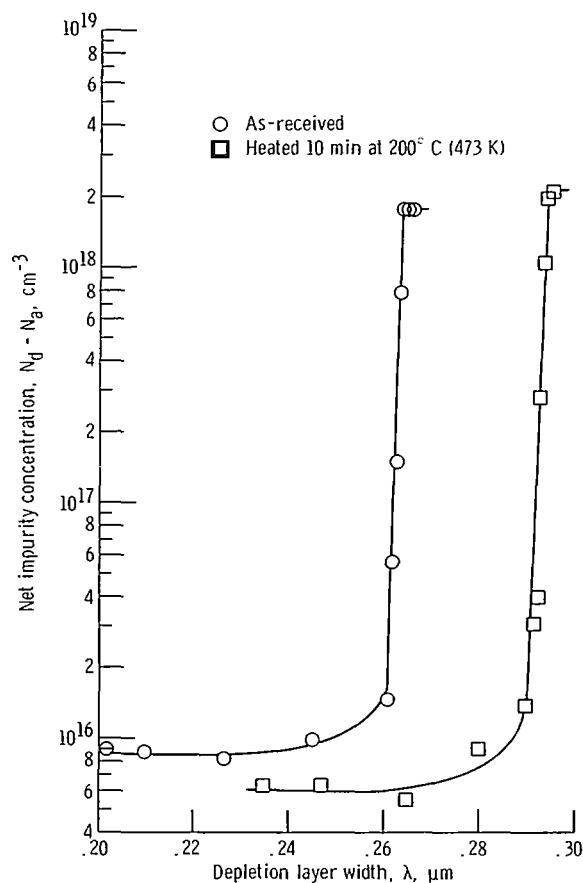


Figure 5. - Effect of heat treatment on impurity distribution in cadmium sulfide layer of cell B724A-6.

## Optical Effects

In addition to acting as compensating centers and deep traps (1.2 eV below the conduction band, ref. 22), copper centers in CdS are also optically active (refs. 5, 8, 10, and 22). The optical and electrical response of these copper centers is strongly influenced by the wavelength of light used to illuminate them (ref. 10). It was of interest, therefore, to determine the effect of various wavelengths of light on the impurity distribution. The light sources and their intensities used in this study were as follows:

| Light      | Source                                                                    | Intensity,<br>mW/cm <sup>2</sup> |
|------------|---------------------------------------------------------------------------|----------------------------------|
| Infrared   | Microscope illuminator with Wratten<br>No. 87 filter (0.8 to 1.2 $\mu$ m) | 10                               |
| White      | Microscope illuminator                                                    | 20                               |
| Blue-green | Hydrogen lamp with 0.498- $\mu$ m<br>monochromatic interference<br>filter | 5                                |

The results are shown in figure 6. In darkness, a distribution similar to that shown in figure 4, which is typical of all cells tested, was obtained. When infrared light illuminated the cell, no substantial change was observed in this distribution. (The slight shift in the curve can be attributed to a small amount of visible light transmitted by the Wratten No. 87 filter.) When white or blue-green light was used to illuminate the cell, substantial changes occurred in the amount of compensation of the CdS:Cu layer. Furthermore, the capacitance measurements were stable at all bias levels and showed no tendency to drift.

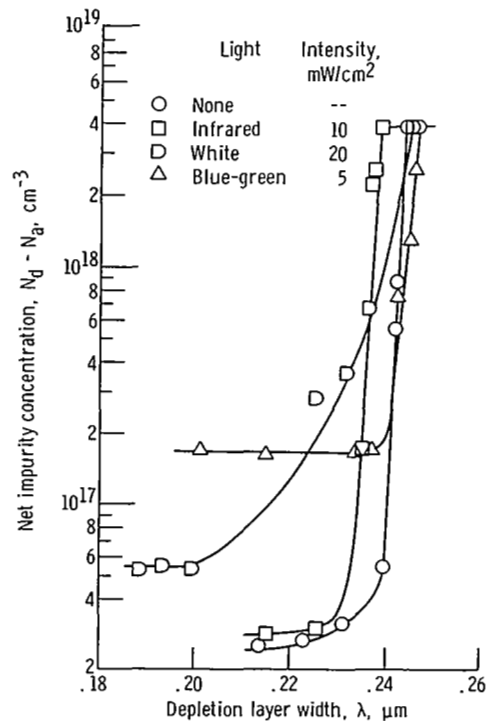


Figure 6. - Effect of illumination on impurity distribution in cadmium sulfide layer of cell B724A-1.

## Electron Microprobe

The impurity profile in the  $\text{Cu}_2\text{S}$  layer was also determined. Hall measurements on thin  $\text{Cu}_2\text{S}$  layers yielded an average value for the carrier concentration of about  $10^{20}$  per cubic centimeter. Because capacitance measurements could not be used and the layer was too thin to profile by known assaying methods, the impurity distribution in the  $\text{Cu}_2\text{S}$  layer was inferred from electron-beam microprobe analyses on thicker layers of  $\text{Cu}_2\text{S}$ . Microprobe analyses were made on a  $\text{Cu}_2\text{S}$ -CdS heterojunction in which the  $\text{Cu}_2\text{S}$  had been chemically formed on single-crystal CdS with the standard chemical dip. These analyses showed a cadmium gradient extending into the  $\text{Cu}_2\text{S}$  for a distance of 10 micrometers. The total thickness of the  $\text{Cu}_2\text{S}$  layer on the CdS single crystal was 190 micrometers. No attempt was made to determine the effect of heat treatment on the depth of the cadmium gradient extending into the  $\text{Cu}_2\text{S}$  layer.

## DISCUSSION

As noted in a previous section, a gradual decay of the applied bias voltage with time occurred. Over a period of hours, the forward voltage decreased from about 1 volt to between 0.4 and 0.6 volt. Decay phenomenon of this type are not necessarily new (refs. 20 and 23) and are thought to be caused by either highly mobile ions or trapping centers located in the depletion region. In the present case, if traps were responsible for the effect, they were probably copper centers. A positive bias would tend to fill these centers completely, because some of them are initially above the Fermi level (ref. 19).

Because no significant change in capacitance was observed during this voltage decay, it is probable that no change took place in the net impurity concentration or in the depth of the compensated layer. However, if the decay in voltage had been caused by the motion of copper ions in the CdS, it is possible that the impurity profile could have been changed. The motion of copper ions may also help to explain the large number of cell failures under forward bias. Further experiments are required to clarify these hypotheses, however.

High field injection might also possibly be responsible for the behavior of the capacitance-voltage plots in the forward direction. If this were true, it would suggest that the impurity concentrations measured for the CdS:Cu region are upper limits. Two factors, however, tend to refute this possibility. First, a plot of the logarithm of the capacitance against the logarithm of the current had a slope of  $1/2$ , which would be expected from equation (1), and not a slope of 2, which would have indicated the presence of high injection. Second, as heat treatments were continued, the compensation of the

CdS:Cu layer also increased, which would not be expected if the forward voltage results were caused by injection. Therefore, in view of these considerations, a band structure for the  $\text{Cu}_2\text{S}$ -CdS heterojunction is assembled in the following section.

## Band Structure of Cuprous Sulfide - Cadmium Sulfide Heterojunction

Based on the impurity profile in the CdS layer determined by capacitance measurements, the carrier concentration in the  $\text{Cu}_2\text{S}$  layer determined by Hall measurements and the electron microprobe data, a band structure can be assembled for the  $\text{Cu}_2\text{S}$ -CdS heterojunction. The heterojunction apparently consists of four regions shown schematically in figure 7: (1) bulk CdS, (2) Cu-doped CdS, (3) Cd-doped  $\text{Cu}_2\text{S}$ , and (4) near-degenerate  $\text{Cu}_2\text{S}$ .

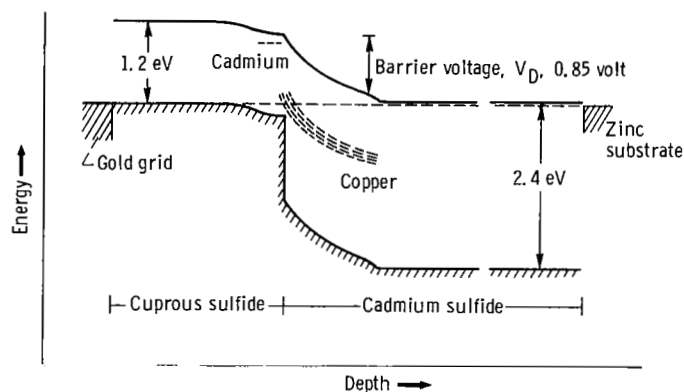


Figure 7. - Band structure for cuprous sulfide-cadmium sulfide heterojunction.

## Bulk Cadmium Sulfide

The bulk CdS is n-type because of excess Cd and has a carrier concentration of about  $10^{18}$  per cubic centimeter. For consistency, all data for the CdS layer are based on the impurity concentrations determined by capacitance measurements (These concentrations may be as much as one order of magnitude too high because of errors in cell area determination, as discussed in the section Impurity Distribution). The depth of the Fermi level below the conduction band edge  $E_f$  was determined from the following equation (ref. 24):

$$E_g - E_f = kT \ln \frac{2}{n} \left( \frac{2\pi m^* kT}{h^2} \right)^{3/2} \quad (3)$$

where  $E_g$  is the band gap,  $k$  is Boltzmann's constant,  $T$  is absolute temperature,  $n$  is the carrier concentration,  $m^*$  is the electron effective mass (for CdS,  $m^* = 0.18 m_0$ , where  $m_0$  is the free electron mass), and  $h$  is Planck's constant. Substitution yields a value of about 0.02 eV. (If the cell area were three times greater, the impurity concentration would be  $2 \times 10^{17}$  per cubic centimeter with a Fermi level depth of 0.06 eV.) The thickness of the bulk CdS is about 25 micrometers (ref. 15).

### Copper-Doped Cadmium Sulfide

As a result of the fabrication heat treatment (2 min at 250° C or 523 K), copper diffuses into the CdS for a distance of about 0.3 micrometer, partially compensating the excess cadmium carriers present there, as shown in figure 4. The impurity concentration in this region is about  $10^{16}$  per cubic centimeter with a Fermi level calculated from equation (3) to be 0.13 eV below the conduction band edge. (Again, increasing the area three times yields  $N_d = \sim 10^{15} \text{ cm}^{-3}$  and  $E_f = 0.19 \text{ eV}$  below the conduction band edge.) The amount of band bending in the n-CdS:Cu is given by the barrier voltage  $V_D$  which averages 0.85 eV. (The values obtained in this study ranged from 0.82 to 0.88 eV.) This value for the barrier height has also been substantiated by optical and capacitance measurements on undiffused  $\text{Cu}_2\text{S}$ -CdS heterojunctions (ref. 16).

### Cadmium-Doped Cuprous Sulfide

As shown by the electron microprobe analysis of the  $\text{Cu}_2\text{S}$ -CdS junction on the CdS single crystal, apparently a region in the  $\text{Cu}_2\text{S}$  layer exists which contains a considerable concentration of cadmium. Although no direct measurements were made to detect such a layer in the polycrystalline film cell used in this study, its existence seems likely. Some general remarks can be advanced as to its nature. Because of the similarity of the sulfur atom packing in both  $\text{Cu}_2\text{S}$  and CdS and because of the fact that copper is a compensating impurity in CdS, it is probable that cadmium acts as a compensating impurity in  $\text{Cu}_2\text{S}$ . Cadmium in the near-degenerate  $\text{Cu}_2\text{S}$  would then raise the Fermi level above the valence band in this region. The height of the Fermi level above the valence band in this region (0.2 eV) has been estimated from the difference between the band gap of  $\text{Cu}_2\text{S}$  (1.2 eV) and the sum of the barrier height for the Cu-doped CdS

(0.85 eV) and the depth of the Fermi level below the conduction band (0.13 eV). If the hole effective mass is assumed to be about  $0.5 m_0$ , a carrier concentration of about  $10^{16}$  per cubic centimeter is obtained from equation (3).

The existence of this  $\text{Cu}_2\text{S}:\text{Cd}$  region does not invalidate the Schottky barrier assumption or the  $A^2/C^2$  analysis of the data. Experimentally, the  $\text{Cu}_2\text{S}:\text{Cd}$  region would be observed in the capacitance study only at high forward voltages. These voltages could not be achieved because at a forward voltage higher than 0.6 volt, cell failure usually occurred as a result of high current flow.

## Cuprous Sulfide Layer

The cuprous sulfide is near-degenerate with a carrier concentration of about  $10^{20}$  per cubic centimeter as determined from Hall effect measurements (ref. 16). Under these conditions, the Fermi level is essentially pinned at the valence band edge. The maximum thickness of the  $\text{Cu}_2\text{S}$  layer is approximately 0.5 micrometer.

The band structure shown in figure 7 does not include possible discontinuities at the  $\text{Cu}_2\text{S}:\text{CdS}$  interface, as discussed by Anderson (ref. 18), because the necessary values of electron affinity, work function, and dielectric constant for  $\text{Cu}_2\text{S}$  are not available.

## Implications of Band Structure and Additional Supporting Evidence

Three major features of the band structure shown in figure 7 can be tested experimentally. First, the optical activity of the copper centers in the CdS can be measured. Second, direct photoexcitation of electrons across the band gap of  $\text{Cu}_2\text{S}$  should be observed. Third, the band structure suggests certain limits on the maximum voltage of the heterojunction and its temperature dependence. It is of interest, then, to discuss these topics.

Optical response of copper centers in cadmium sulfide. - In addition to acting as compensating centers and deep traps, copper centers in CdS are also optically active. Illumination of the CdS with blue-green light (or other strongly absorbed radiation) generates holes that are captured by these copper centers (refs. 8, 9, and 22). These new centers (presumably  $\text{Cu}^{2+}$ ) are not compensating centers; hence, the amount of compensation in the  $\text{CdS}:\text{Cu}$  region should be reduced. Figure 6 shows that the amount of compensations has indeed decreased under blue-green illumination; however, the light intensities that were used in this study were not high enough to eliminate the compensating centers completely. Also, under blue-green or white illumination,  $\text{Cu}^{2+}$  does not act as a trapping center, presumably because it is below the Fermi level in the depletion region.

Accordingly, no rise or decay in output typical of the behavior of trapping centers was observed in the capacitance measurements under blue-green or white light. Red light, however, had no effect on the impurity profile nor did it after the transient changes in output typical of trapping centers.

Furthermore, because strongly absorbed light reduces the amount of compensation of the CdS, it should also reduce the series resistance of the cell. From the data of figure 6, one can see that the series resistance of the cell in red light should be greater than the resistance in blue-green or white light. This higher resistance in red light has been experimentally observed to be the case (ref. 10).

Photoresponse of cuprous sulfide. - It is doubtful that the strong infrared light absorption of these copper centers (ref. 8) in the CdS can contribute to the red response of the cell because only holes are involved in the transitions. However, the red response of the cell could possibly come from photon absorption which would lead to hole-electron-pair formation in the  $\text{Cu}_2\text{S}$  (ref. 10). In support of this possibility, the absorption coefficient and band gap for  $\text{Cu}_2\text{S}$  (ref. 25) indicate that significant red response can indeed be generated by this layer at thicknesses less than 0.5 micrometer. Therefore, the low energy threshold of the spectral response of the cell should then occur at 1.2 eV. Strong evidence supporting these suggestions has been obtained experimentally (refs. 10 and 16).

Maximum cell voltage. - To a first approximation, the maximum open-circuit voltage that can be obtained from a heterojunction should be determined by the material with the smallest band gap (ref. 26). That the smaller band gap material largely determines the voltage helps to explain why the magnitude of the voltage and its temperature coefficient (ref. 27) in the  $\text{Cu}_2\text{S}$ -CdS heterojunction resemble the silicon solar cell (silicon band gap, 1.1 eV,  $\text{Cu}_2\text{S}$  band gap, 1.2 eV). From the band structure determined for the cells used in this study, the maximum open-circuit voltage should approximate the barrier height of about 0.85 volt. Under 1-sun illumination, a maximum open-circuit voltage of 0.7 volt has been observed at about  $-123^\circ\text{C}$  (150 K) on similar thin-film  $\text{Cu}_2\text{S}$ -CdS heterojunctions (unpublished data obtained from C. H. Liebert of the NASA Lewis Research Center). It is felt that if cells with much higher shunt resistances were available, closer agreement to the 0.85-eV barrier would be obtained.

## SUMMARY OF RESULTS

Capacitance-voltage measurements were made on cuprous sulfide-cadmium sulfide ( $\text{Cu}_2\text{S}$ -CdS) heterojunctions formed by acid etching an evaporated polycrystalline CdS layer and dipping it into a cuprous ion solution. The net impurity profile in the CdS layer was determined from the capacitance measurements. These measurements showed that the copper which was diffused into the CdS during a fabrication heat treat-



ment did not completely compensate the excess cadmium centers in the CdS but did reduce the impurity concentration between two and three orders of magnitude. The barrier height was determined to be 0.85 volt, which represents the maximum voltage that can be obtained with this heterojunction.

On the basis of the impurity profile determined from capacitance measurements and Hall and electron microprobe measurements on the  $\text{Cu}_2\text{S}$ , a band structure for the  $\text{Cu}_2\text{S}$ -CdS heterojunction was assembled. Four regions were apparently present in the device: (1)  $n^+$ -type CdS, donor impurity concentration ( $N_d$ ) of approximately  $10^{18}$  per cubic centimeter, Fermi level 0.02 eV below the conduction band edge; (2) n-type CdS:Cu,  $N_d$  of approximately  $10^{16}$  per cubic centimeter, Fermi level 0.13 eV below the conduction band edge; (3) p-type  $\text{Cu}_2\text{S}$ :Cd, acceptor impurity concentration ( $N_a$ ) approximately equal to  $10^{16}$  per cubic centimeter, Fermi level about 0.2 eV above the valence band edge; and (4)  $p^+$ -type  $\text{Cu}_2\text{S}$ ,  $N_a$  of approximately  $10^{20}$  per cubic centimeter, near-degenerate  $\text{Cu}_2\text{S}$ , Fermi level at the valence band edge.

The effects of various wavelengths of light on the amount of compensation in the CdS:Cu layer were studied. The amount of compensation did not change from its dark value when irradiated with infrared light, but blue-green or white light considerably reduced the degree of compensation of the CdS, which indicated the optical activity of the copper centers.

This band structure and other published data suggest that most of the red response comes from the  $\text{Cu}_2\text{S}$  layer and that the maximum voltage of the heterojunction is limited to about 0.85 volt.

Lewis Research Center,  
National Aeronautics and Space Administration,  
Cleveland, Ohio, December 12, 1968,  
120-33-01-09-22.

## REFERENCES

1. Reynolds, D. C.; Leies, G.; Antes, L. L.; and Marburger, R. E.: Photovoltaic Effect in Cadmium Sulfide. *Phys. Rev.*, vol. 96, no. 2, Oct. 15, 1954, pp. 533-534.
2. Reynolds, D. C.; and Czyzak, S. J.: Mechanism for Photovoltaic and Photoconductivity Effects in Activated CdS Crystals. *Phys. Rev.*, vol. 96, no. 6, Dec. 15, 1954, p. 1705.
3. Woods, J.; and Champion, J. A.: Hole Conduction and Photovoltaic Effects in CdS. *J. Electronics and Control*, vol. 7, 1959, pp. 243-253.

4. Williams, Richard; and Bube, Richard H.: Photoemission in the Photovoltaic Effect in Cadmium Sulfide Crystals. *J. Appl. Phys.*, vol. 31, no. 6, June 1960, pp. 968-978.
5. Grimmeiss, H. G.; and Memming, R.: p-n Photovoltaic Effect in Cadmium Sulfide. *J. Appl. Phys.*, vol. 33, no. 7, July 1962, pp. 2217-2222.
6. Grimmeiss, H. G.; and Memming, R.: Origins of the Photovoltaic Effect Vapor-Deposited CdS Layers. *J. Appl. Phys.*, vol. 33, no. 12, Dec. 1962, pp. 3596-3597.
7. Fabricius, E. D.: Photoeffect in Au-CdS and Cu-CdS Photovoltaic Cells. *J. Appl. Phys.*, vol. 33, no. 4, Apr. 1962, pp. 1597-1603.
8. Duc Cuong, N.; and Blair, J.: Impurity Photovoltaic Effect in Cadmium Sulfide. *J. Appl. Phys.*, vol. 37, no. 4, Mar. 15, 1966, pp. 1660-1669.
9. Palz, W.; and Ruppel, W.: Minority Carriers in CdS. I. Photovoltage for Optical Excitation Inside and Outside of Eigen Absorption Considered as a Minority Carrier Effect. *Physica Status Solidi*, vol. 15, 1966, pp. 649-663.
10. Potter, Andrew E., Jr.; Berry, William B.; Brandhorst, Henry W., Jr.; and Schalla, Rose L.: Effect of Green Light on Spectral Response of Cuprous Sulfide - Cadmium Sulfide Photovoltaic Cells. NASA TN D-4333, 1968.
11. Bockemuehl, Robert R.; Kauppila, James E.; and Eddy, David S.: Analysis of Photojunctions Formed by Diffusing Copper into Insulating Cadmium Sulfide Crystals. *J. Appl. Phys.*, vol. 32, no. 7, July 1961, pp. 1324-1330.
12. Cusano, D. A.: CdTe Solar Cells and Photovoltaic Heterojunctions in II-VI Compounds. *Solid State Elec.*, vol. 6, no. 3, May-June 1963, pp. 217-232.
13. Keating, P. N.: Hole Injection into CdS from Cu<sub>2</sub>S. *J. Phys. Chem. Solids*, vol. 24, 1963, pp. 1101-1106.
14. Keating, P. N.: Photovoltaic Effect in Photoconductors. *J. Appl. Phys.*, vol. 36, no. 2, Feb. 1965, pp. 564-570.
15. Shirland, Fred A.: The History, Design, Fabrication and Performance of CdS Thin Film Solar Cells. *Adv. Energy Conversion*, vol. 6, no. 4, Oct.-Dec. 1966, pp. 201-222.
16. Potter, Andrew E., Jr.; and Schalla, Rose L.: Mechanism of Cadmium Sulfide Film Cell. NASA TN D-3849, 1967.
17. Schottky, W.: Vereinfachte und Erweiterte Theorie der Randschichtgleichrichter. *Zeit. f. Physik*, vol. 118, no. 9-10, Feb. 1, 1942, pp. 539-592.

18. Anderson, R. L.: Experiments on Ge-GaAs Heterojunctions. Solid State Elect., vol. 5, Sept.-Oct. 1962, pp. 341-351.
19. Goodman, Alvin M.: Metal-Semiconductor Barrier Height Measurement by the Differential Capacitance Method - One Carrier System. J. Appl. Phys., vol. 34, no. 2, Feb. 1963, pp. 329-338.
20. Henisch, Heinz K.: Rectifying Semi-conductor Contacts. Oxford Univ. Press, 1957.
21. Aven, M.; and Halsted, R. E.: Diffusion of Electrically and Optically Active Defect Centers in II-IV Compounds. Phys. Rev., vol. 137, no. 1A, Jan. 4, 1965, pp. A228-A234.
23. Morigaki, Kazuo: Electron Spin Resonance of a Photosensitive Center in Cu doped CdS. J. Phys. Soc. Japan, vol. 19, no. 7, July 1964, p. 1240.
24. Williams, Richard: Determination of Deep Centers in Conducting Gallium Arsenide. J. Appl. Phys., vol. 37, no. 9, Aug. 1966, pp. 3411-3416.
24. Kittel, Charles: Introduction to Solid State Physics. Third ed., John Wiley & Sons, Inc., 1966.
25. Marshall, R.; and Mitra, S. S.: Optical Properties of Cuprous Sulfide. J. Appl. Phys., vol. 36, no. 12, Dec. 1965, pp. 3882-3883.
26. Wolf, M.: Limitations and Possibilities for Improvement of Photovoltaic Solar Energy Converters. Part I: Considerations for Earth's Surface Operation. Proc. IRE, vol. 48, no. 7, July 1960, pp. 1246-1263.
27. Wysocki, Joseph J.; and Rappaport, Paul: Effect of Temperature on Photovoltaic Solar Energy Conversion. J. Appl. Phys., vol. 31, no. 3, Mar. 1960, pp. 571-578.